Soft Matter

Cite this: *Soft Matter*, 2012, **8**, 11905

www.rsc.org/softmatter

PAPER

Shape as a determinant of membrane protein cluster formation

Diana Morozova, Matthias Weiss and Gernot Guigas*

Received 25th July 2012, Accepted 14th September 2012
DOI: 10.1039/c2sm26720a

Cluster formation of membrane proteins is a crucial event in many vital cellular processes. Here, we present a thorough examination of the oligomerisation ability of membrane proteins with different geometries. By means of mesoscopic membrane simulations we show that lipid-mediated interactions between proteins depend both on the shape of the hydrophobic domain of the proteins and on their hydrophobic mismatch. Based on that, we find that protein interactions can be either attractive or repulsive, depending on the characteristic bilayer perturbations induced by the proteins. The influence of these perturbations is quantified *via* the associated potential of mean force. Such geometry-dependent interactions are likely to fine-tune protein oligomerization events during cellular processes, for example signal transduction or protein sorting.

Introduction

A multitude of biological processes, ranging from signal transduction to protein sorting, depend on the formation of membrane protein clusters. In many cases it is unknown whether these clusters are formed due to specific chemical bonds, or whether their assembly is driven by unspecific interactions. Biophysical studies have emphasized the importance of membrane-mediated interactions in this context. Such interactions were ascribed, for instance, to elastic deformations of the membrane,[1–4] perturbations of the conformational freedom of lipids,[5–7] wetting effects,[8] membrane curvature,[9,10] capillary forces,[11] or membrane fluctuations.[12–15]

In particular, protein attraction due to a hydrophobic mismatch has been studied in some detail. The term 'hydrophobic mismatch' denotes a length difference between the hydrophobic domain of a transmembrane protein and the hydrophobic thickness of the host lipid bilayer. Theoretical predictions of protein clustering due to a hydrophobic mismatch (*e.g.* ref. 1–3) are supported by experiments[16–19] as well as simulations.[7,20–23]

In these studies, however, typically cylindrically shaped proteins are assumed, whereas in reality many membrane proteins deviate from a pure cylindrical form.[24,25] Bearing in mind that unspecific interactions often arise from membrane perturbations, it is tempting to assume that interactions induced by non-cylindrical proteins may differ profoundly from those induced by cylinders. Moreover, for non-cylindrical entities significant interactions may be expected even in the absence of a hydrophobic mismatch. Mean-field theories indeed predict for non-cylindrical proteins the possibility of both mutual repulsion and attraction.[25,26]

Experimental Physics I, University of Bayreuth, Bayreuth, Germany. E-mail: gernot.guigas@uni-bayreuth.de

Here, we have investigated the influence of protein shape on non-specific interactions between membrane proteins by means of coarse-grained computer simulations. We have studied two axially symmetric transmembrane protein types which deviate in shape from a cylinder: 'barrel-shaped' proteins with convex form, and 'hourglass-shaped' proteins with a concave body. We calculated the potential of mean force for protein pairs with different hydrophobic mismatches and found that deviating from a cylindrical shape can turn the effect of hydrophobic mismatch from attraction to pure repulsion. To understand the origin of these interactions, we monitored local perturbations of the membrane induced by proteins. In line with our expectations, we observed that protein clustering reduced the perturbations in cases of attraction. In contrast, approach of proteins would even increase the membrane perturbations in cases of repulsion. Thus, we found that the shape of the hydrophobic domain of the proteins and their hydrophobic mismatch are both crucial parameters determining membrane-mediated interactions of proteins.

Methods

To study the interactions of membrane proteins, we have used Dissipative Particle Dynamics (DPD), a standard simulation model for complex fluids and membranes.[27–29] Similar to molecular dynamics, DPD is based on the motion and interaction of single particles moving according to Newton's laws. In DPD, single particles represent groups of atoms, which were in our case water (W), hydrophilic groups (H) and hydrophobic groups (T). This coarse-grained modelling has two advantages for our study: On the one hand it allows us to access larger time and length scales than more detailed models (at the expense of neglecting atomic details and electrostatics). On the other hand it takes into account only hydrophobic and hydrodynamic interactions, *i.e.* it allows one to focus on the generic geometric interactions.

In our simulations, two particles i and j interact *via* three pairwise forces $\boldsymbol{F}_{ij}^{C}$, $\boldsymbol{F}_{ij}^{D}$, $\boldsymbol{F}_{ij}^{R}$ when their distance $r_{ij} = |r_{ij}| = |r_i - r_j|$ is smaller than a cutoff distance r_0 which sets the length unit of the simulation. A conversion of the simulation units to SI units yields $r_0 \approx 1$ nm and $\Delta t \approx 100$ ps; technical details may be found in ref. 7. The degree of hydrophobicity of the beads is set *via* the repulsive force $\boldsymbol{F}_{ij}^{C} = a_{ij}(1 - r_{ij}/r_0)\hat{\boldsymbol{r}}_{ij}$, using interaction energies $a_{WW} = a_{WH} = a_{HH} = a_{TT} = 25k_BT/r_0$ and $a_{WT} = a_{HT} = 200k_BT/r_0$.[30] The dissipative force $\boldsymbol{F}_{ij}^{D} = -\gamma(1 - r_{ij}/r_0)^2(\hat{\boldsymbol{r}}_{ij}\cdot\boldsymbol{v}_{ij})\hat{\boldsymbol{r}}_{ij}$ is coupled with the random force $\boldsymbol{F}_{ij}^{R} = \sigma(1 - r_{ij}/r_0)\xi_{ij}\hat{\boldsymbol{r}}_{ij}$ to a thermostat *via* the fluctuation–dissipation theorem $\gamma = \sigma^2/(2k_BT)$ with $\gamma = 4.5\sqrt{k_BTm}/r_0$, $\sigma = 3((k_BT)^3m/r_0^2)^{1/4}$. The parameter $\boldsymbol{v}_{ij} = \boldsymbol{v}_i - \boldsymbol{v}_j$ is the relative velocity of the two interacting beads, while ξ_{ij} is an uncorrelated random variable with zero mean and unit variance. All types of DPD particles in the simulation had the same mass m.

Lipids were modelled as linear chains consisting of one hydrophilic and three hydrophobic beads HT_3 (Fig. 1a). Bead connections were implemented as Hookean springs, *i.e.* two succeeding beads i,i + 1 were connected by an attractive harmonic potential $U_{harm}(r_i,r_{i+1}) = k_{harm}(r_{i,i+1} - l_0)^2/2$, with spring stiffness $k_{harm} = 100k_BT/r_0^2$ and the equilibrium bond length $l_0 = 0.45r_0$. Strong bending of lipid chains was prevented by a three-point bending potential $U_{stiff}(r_{i-1},r_i,r_{i+1}) = k_{stiff}(1 - \cos(\theta))$, with the bond angle $\cos(\theta) = \hat{\boldsymbol{r}}_{i-1,i}\cdot\hat{\boldsymbol{r}}_{i,i+1}$ (bending constant $k_{stiff} = 10k_BT$). An equilibrated tensionless bilayer of these lipids had a thickness of 3.5 nm (Fig. 1e).

Transmembrane proteins had a hydrophilic top consisting of bead type H, a hydrophobic domain with a length of n layers consisting of bead type T and a hydrophilic bottom consisting of bead type H (Fig. 1b). The cross-section of a cylinder was a hexagon with a diagonal of $2k - 1$ beads, *i.e.* the parameter k determined the protein radius. In the vertical direction the beads were ordered in chains. For cylindrical proteins we used $k = 3$, which corresponds to a radius $R \approx 1$ nm. In barrel-shaped and hourglass-shaped proteins the radii k of the layers varied along the rotation axis of the protein. Barrels had a small radius $k = 1$ at their top and bottom, and a maximal radius $k = 4$ at their middle part, corresponding to $R_{max} \approx 1.5$ nm (Fig. 1c). Hourglasses had a large radius $k = 4$ at their top and bottom, and a minimal radius $k = 2$ at the middle part (Fig. 1d). All protein types were studied with two different lengths $n = 3$ and $n = 6$ of the hydrophobic domain, which correspond to hydrophobic mismatches of −1 nm and +1 nm, respectively. Each bead of a protein was linked to all next neighbor beads (maximally six) within the protein cross-section and to its two direct neighbor beads in the sections above and below. Beads were linked using the potential $U_{harm}(r_i,r_{i+1})$. Furthermore, $U_{stiff}(r_{i-1},r_i,r_{i+1})$ was used to maintain the rigidity of vertical chains consisting of three or more beads. The potential settings were the same as for lipids. Due to this construction, proteins were relatively rigid objects with a negligible internal flexibility. During a simulation, proteins deviated less than 5% from a perfectly rigid cylindrical backbone, as quantified *via* the bending angle between protein top, middle and bottom.

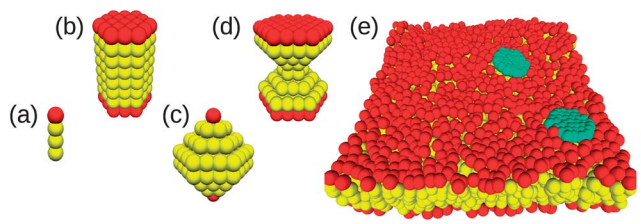

Fig. 1 Simulation setup. (a) Model lipid with a hydrophilic head group (red in the online version, dark in the print version) and three hydrophobic tail groups (yellow/light). (b–d) Models of transmembrane proteins with hydrophilic top and bottom (red/dark), and a hydrophobic middle section (yellow/light). We probed three different protein shapes: cylindrical (b), barrel-like (c) and hourglass-like (d). (e) Snapshot of a lipid membrane hosting two hourglass-shaped proteins (displayed in light green); water beads are not shown for better visibility.

The particle density of the entire system was 3 beads per r_0^3. Equations of motion were integrated with a modified Velocity Verlet algorithm,[28] using periodic boundary conditions and a time increment $\Delta t = 0.01\sqrt{mr_0^2/k_BT}$. Please note that integration of the forces $\boldsymbol{F}_{ij}^{R}$ requires a factor $\sqrt{\Delta t}$, whereas $\boldsymbol{F}_{ij}^{C}$ and $\boldsymbol{F}_{ij}^{D}$ have a factor Δt.

The potential of mean force of two proteins, $U(r)$, was determined from the distribution $P(r)$ of the two-dimensional center-of-mass distances r of the proteins with the relation $U(r) = -k_BT\ln(P(r))$. A uniform sampling of the entire configurational space was achieved using the umbrella sampling method.[31,32] For umbrella sampling, r was restricted to windows by harmonic potentials $V_i(r) = K_{umbr}(r - d_i)^2/2$ with centers $d_i = 0.5,\ldots,9.5$. For each window i, the system was equilibrated for 2×10^5 time steps with a barostat[33] to achieve a tensionless bilayer ($N\sigma T$ ensemble, where σ is the surface tension). Then the equilibrated system size was fixed to the NVT ensemble and r was recorded during the following 5×10^5 time steps. Unbiasing and combining the distributions $P_i(r)$ of each window with the weighted histogram analysis method (WHAM) yielded $P(r)$. A more detailed description of the approach can be found in ref. 20.

Tests with different system sizes showed that the potential of mean force of two proteins had reproducibly the same shape when the linear size of a membrane patch was >20 nm. For smaller patches the potential showed modifications depending on the system size, *e.g.* a deeper minimum of the potential well. In all simulations presented in this paper we have therefore chosen a box size of 30 nm × 30 nm × 15 nm which is sufficiently large to avoid finite size effects.

Results

Potential of mean force for different protein pairs

As a first step to quantitatively characterize membrane-mediated interactions between proteins with different shapes and hydrophobic mismatches, we have determined the potential of mean force (PMF) between two proteins, embedded in a membrane patch of linear size $L = 30$ nm. As a baseline, we first probed two identical cylindrical proteins with a radius $R = 1$ nm (Fig. 1b). We observed deep minima in the PMF upon contact of the cylinders, which indicates mutual attraction (Fig. 2a). The binding energy ΔE is given by the depth of the potential minimum as compared to the potential value at large separation distances. In agreement with earlier simulation studies,[7] we found $\Delta E \approx 8k_BT$ for both a positive and a negative hydrophobic mismatch (±1 nm).

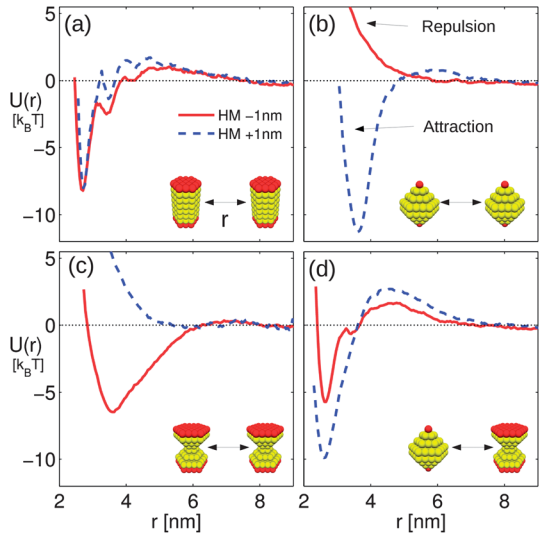

Fig. 2 Potential of mean force $U(r)$ for two membrane proteins at a center-of-mass distance r. A pronounced local minimum of $U(r)$ indicates attraction, while local maxima indicate repulsion. (a) We have observed mutual attraction between two cylinders, both for a positive (+1 nm) and a negative hydrophobic mismatch (−1 nm). (b) For two barrels, we found attraction only for a positive mismatch (blue dashed curve), but repulsion for a negative mismatch (red full line). (c) For two hourglasses, we observed repulsion for a positive (blue dashed line), but attraction for a negative mismatch (red full line). (d) A barrel and an hourglass attract each other for any mismatch. Additional features of the potentials are discussed in the main text.

Next, we probed transmembrane proteins that deviated from a cylindrical shape. We explored two axially symmetric protein types: a convex shape ('barrel', Fig. 1c), and a concave shape ('hourglass', Fig. 1d). These proteins had a maximum radius $R_{max} = 1.5$ nm at their widest radial cross-section. Our simulations showed that for both protein types the character of interaction changed massively as compared to cylinders. Indeed, attraction as well as repulsion regimes emerged, depending on the hydrophobic mismatch of the proteins. Two barrel-like proteins attracted each other when they both had a negative hydrophobic mismatch (binding energy $\Delta E \approx 11 k_B T$), but repelled each other when they both had a positive mismatch (Fig. 2b). Two hourglass-like proteins showed the opposite effect, *i.e.* they repelled each other for a positive mismatch, but attracted each other for a negative one ($\Delta E \approx 6 k_B T$) (Fig. 2c). In both cases, the PMF, $U(r)$, showed a pronounced minimum upon contact of the proteins in the case of attraction, and a steep increase for small inter-protein distances in the case of repulsion. To complement our results, we also tested the interaction of a barrel with an hourglass of identical length. Here we found mutual attraction for a positive and a negative hydrophobic mismatch ($\Delta E \approx 10 k_B T$ and $6 k_B T$) (Fig. 2d).

Inspecting the fine structure of the potential of mean force $U(r)$, we observed two side minima for cylindrical proteins besides the main minimum, and a weak repulsive barrier at larger distances. The range of attraction of $U(r)$ was about 2 nm for two cylinders and two barrels with a positive mismatch, while it was clearly enhanced to 3–4 nm for two hourglasses with a negative mismatch. Neither barrels nor hourglasses showed a fine structure with side minima in $U(r)$. For the combination of a barrel and an hourglass, the interaction range was similar to two cylinders and the repulsive barrier was slightly increased (1–$2 k_B T$). To gain an understanding of the observed phenomenology, we next monitored the perturbations of the surrounding lipid bilayer.

Attraction and repulsion are caused by membrane perturbations

To understand the origin of the shape-induced interactions, we have examined the membrane structure with two model proteins. In particular, we studied the reorganization of lipids upon altering the protein distance. To this end, we performed simulations of membranes hosting two proteins that were fixed by a spring potential in a center-of-mass distance of 9 nm. Then, we reduced the fixed distance in steps of 0.5 nm until the proteins were in contact (center-of-mass distance equals protein diameter). We allowed the membrane to equilibrate for the chosen distance and characterized the membrane structure *via* the density of hydrophobic lipid chains, ρ, *i.e.* the number of lipid chains per area. We monitored ρ for different protein shapes and hydrophobic mismatches (*cf.* Fig. 3).

Our simulations showed that membranes were locally perturbed near the embedded proteins. The chain density ρ was significantly increased or reduced in annular layers around the proteins, as compared to the average value $\rho \approx 3.1$ nm^{-2} in an unperturbed membrane (*e.g.* far away from the proteins). All pictures on the left in Fig. 3a–f display ρ for membranes with proteins at a distance of 5 nm. The layers of altered ρ values around the proteins are clearly visible, with character and range of the perturbation being dependent on the protein shape and hydrophobic mismatch.

As a main result, we have found that protein interactions are a consequence of lipid reorientation upon reduction of the protein distance. Lipids between the proteins are exposed to the influence of both proteins and rearrange their position and orientation dependent on the protein distance. As a consequence, attraction or repulsion of the proteins emerges, reflected by a decay or a rise of the potential of mean force. Attraction was observed when the lipid reorganisation led to a decrease of the total perturbation of the membrane. In other words, a transition to an energetically more beneficial membrane configuration was achieved. In contrast, repulsion was observed when the lipid reorganisation amplified the perturbations in the membrane, which is energetically unfavorable.

Comparing different protein shapes, we found always attraction when two proteins established a maximum interfacial contact by adsorbing to each other along the full length of their hydrophobic domains. This holds for two cylinders (Fig. 3a and b) and for the combination of a barrel and an hourglass. When adsorbing to each other, the hydrophobic portions of the proteins had not to be covered with lipid chains at the contact area (Fig. 3a and b). Hence clustering of the proteins (and coalescing of their lipid annuli) led to a strong reduction of the number of lipids perturbed by the two proteins. Indeed, we found for these protein types, attractive potentials of mean force $U(r)$ with high binding energies of $\Delta E = 6$–$11 k_B T$, both for a positive and a negative hydrophobic mismatch.

In contrast, we observed that protein interaction could be either attractive or repulsive when only a pointwise interfacial

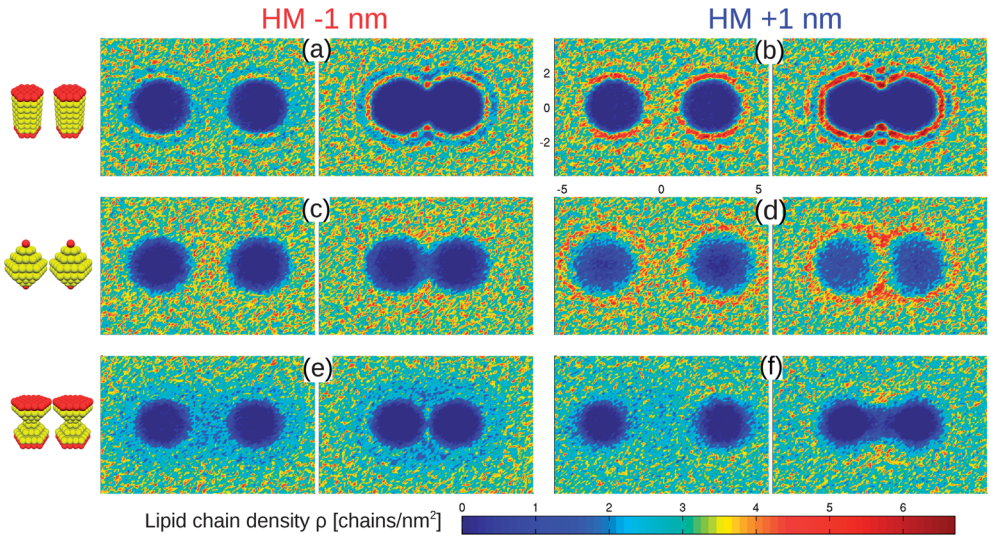

Fig. 3 The lipid chain density ρ in a membrane hosting two proteins (top view). (a) ρ was reduced near to cylinders with a hydrophobic mismatch HM = −1 nm. Upon reduction of the distance between the cylinders, the annuli of reduced ρ coalesced and enclosed both proteins. This caused an attractive protein interaction, since the coalescence decreased the number of perturbed lipids. (b) ρ was increased next to cylinders with HM = +1 nm. Similarly to case (a), the coalescence of the annuli of perturbed ρ caused protein attraction. (c) ρ was moderately increased near to barrels with HM = −1 nm. Upon protein distance reduction, a new region of strongly reduced ρ appeared between the barrels. Such a lipid configuration would be energetically unfavorable for the membrane; therefore, we observed protein repulsion. (d) ρ was strongly increased next to barrels with HM = +1 nm. Upon protein distance reduction, the annuli of perturbed ρ coalesced without emergence of strong new membrane distortions, similarly to case (a). Thus, the protein interaction was attractive. (e) ρ was strongly reduced next to hourglasses with HM = −1 nm. Similarly to case (d), the coalescence of the annuli of perturbed ρ caused protein attraction. (f) ρ was slightly increased near to hourglasses with HM = +1 nm. Similarly to case (c), a new region of strongly reduced ρ appeared between the hourglasses upon protein distance reduction, and proteins repelled each other.

contact of two proteins was possible. This holds for two barrels (Fig. 3c and d) or two hourglasses (Fig. 3e and f), which can touch each other only with the radially most extended parts of their surfaces.

Repulsion was found for two barrels with a negative and two hourglasses with a positive hydrophobic mismatch. When these proteins were set to touching distance, we observed that the lipid chain density ρ was reduced very strongly in the region between the proteins (Fig. 3c and f). Determining the tilting angle ϕ of lipids with the membrane normal yielded values $\phi \approx 0.8$–1.2, as compared to $\phi \approx 0.36$ for unperturbed lipids. In other words, lipids between the proteins had to tilt strongly to cover the hydrophobic domain of the two barrels at their touching point, or to fill the cavity between the two hourglasses with their chains. Such a configuration with a locally very strongly reduced lipid chain density (and increased lipid tilt) would be energetically highly unfavorable for the membrane. As a consequence, we observed for these scenarios a purely repulsive potential $U(r)$.

Mutual attraction was found for two barrels with a positive and two hourglasses with a negative hydrophobic mismatch. When two proteins of these types were in touching distance, ρ had almost the same value in regions between or far away from the two proteins (Fig. 3d and e). In other words, lipids were able to cover the two proteins without experiencing strong distortions, and the approaching of the proteins reduced the number of lipids perturbed by the protein vicinity. Thus, an attractive PMF $U(r)$ of the proteins was found with binding energies $\Delta E = 6$–$11 k_B T$.

Besides attraction or repulsion, the fine structure of the attractive potentials can also be related to the membrane perturbations. For two cylinders, we observed a main minimum and two side minima in the PMF $U(r)$ (Fig. 2a). In agreement with that we also found three maxima and minima in the lipid chain density ρ near the protein (Fig. 3a and b). For other protein shapes we did not see a distinct fine structure either in the potentials or in the chain density.

Discussion

In summary, we have shown that the membrane-mediated interactions of two membrane proteins can be either attractive or repulsive, depending on the three-dimensional shape of the proteins. Two proteins attract each other if their approach is associated with a reorganisation of the membrane leading to an energetically more favorable configuration with reduced membrane perturbations. In contrast, proteins repel each other if their approach enhances the perturbations. Therefore, we always observe attraction when two proteins can establish a maximum interfacial contact by adsorbing to each other along the full length of their hydrophobic domains. In contrast, if only a pointwise interfacial contact is possible, attraction or repulsion may emerge, depending on the hydrophobic mismatch.

These results highlight that caution is necessary when estimating the interactions of two membrane proteins. Using the simplified model of a cylindrical protein shape leads to the prediction that both a positive and a negative hydrophobic mismatch cause attraction.[7,20] However, we have shown here that deviations from the cylinder shape induce a significant change in interaction, meaning that attraction can be strengthened, weakened or even turned into repulsion.

To check the general validity of our findings, we repeated our calculations of $U(r)$ for proteins with reduced radii (cylinders with $R = 0.5$ nm and barrels/hourglasses with $R_{max} = 1$ nm). In all cases, we observed that the character of the interaction (attraction or repulsion) was conserved, while the binding energies varied somewhat. Furthermore we performed simulations with reduced hydrophobic mismatches (HM $= \pm 0.3$ nm). Again we have found that the character of the interactions (attraction/repulsion) did not change, while the binding energies slightly decreased upon reduction of the absolute value of the mismatch.

Our results agree qualitatively very well with mean-field calculations done by May and Ben-Shaul.[25] They predict an attractive interaction for two barrel-shaped membrane proteins with a positive and two hourglass-like proteins with a negative hydrophobic mismatch, but a repulsive interaction between two barrels with a negative and two hourglasses with a positive mismatch, which is exactly what we find in our simulations. Furthermore, attraction between two cylinders is predicted to be independent of the sign of their hydrophobic mismatch, which is confirmed by our simulations. Comparing our simulations in more detail with the mean-field theory, we find for all cases of attraction between proteins (including two cylinders) a repulsive increase of the PMF at the nearest protein–protein distance due to the elasticity of our model proteins. This elasticity feature is not included in the mean-field theory, where proteins are modelled as rigid objects which adsorb to each other without fluctuations of the overlap. In case of attraction of two barrels or two hourglasses, theory predicts a shift of the minimum to a larger inter-protein distance, indicating dimerization with a layer of lipids in between, which we do not observe in the simulations. While we see a significantly wider potential minimum for two hourglasses with negative mismatch compared to cylinders or barrels, this is not predicted by the theory. However, apart from these details which we attribute to the choice of model settings, simulation and theory predict qualitatively the same shape dependence of the interactions of two membrane proteins.

Our results furthermore agree with experimental studies on mismatch-driven clustering of membrane proteins. For membrane-mediated association of transmembrane helices (which can be modelled as cylinders), binding energies between $4k_BT$ and $10k_BT$ were reported,[19] which are well comparable with the typical binding energies found in our simulations. In another study, gramicidin A was observed to form clusters when embedded in a lipid bilayer where it had a negative mismatch.[34] In the clusters the nearest neighbor distance of proteins was larger than the protein diameter, which suggests that the clusters were a lipid–protein mixture. Inspecting the structure of gramicidin A, it would be best represented by an hourglass shape, for which we have observed attraction with a wide potential minimum in case of a negative mismatch. The latter means a probable nearest neighbor distance larger than the protein diameter, which agrees well with the experimental findings. Assuming a cylindrical shape would lead to a prediction of clusters of pure protein with a nearest neighbor distance of the protein diameter.

Generally, our finding of shape-dependent interactions between membrane proteins could be important for biology, biophysics and biotechnology under many aspects. The hydrophobic domains of membrane proteins often deviate in their shape from an ideal cylinder. Therefore when considering their possible interactions, one should not only take into account the hydrophobic mismatch, but their overall geometrical form. The gross shape of a protein may give a first hint if it rather appears as a monomer or a multimer in a cell membrane. A conformational alteration of protein shape, on the other hand, could serve as a switch between a monomeric and a multimeric state. In signaling an extracellular stimulus may induce a conformational change of a membrane receptor from a repulsive to a strongly attractive state (*e.g.* from hourglass to cylinder). The resulting oligomerisation of the receptor would then initiate further propagation of the signal by a second messenger into the cell. As another example, protein sorting could benefit from the shape-driven interactions: Using both hydrophobic mismatch and protein shape as parameters that control nonspecific attraction/repulsion, the cell has a means to regulate the assembly (or exclusion) of a wide range of different proteins without the need of specific interactions. Regarding the variety of protein shapes and the possibility of conformation changes, our findings may explain how nonspecific forces can support clustering of certain proteins without causing hazardous aggregation.

In conclusion, we have shown that membrane-mediated interactions of membrane proteins are determined both by the three-dimensional shape of the transmembrane domain of the proteins and their hydrophobic mismatch with the membrane. Interactions can be either attractive or repulsive, depending on the perturbations of the membrane caused by the proteins. For an experimental test of our predictions, we suggest insertion of well-characterized fluorescently labeled proteins of different shapes, *e.g.* gramicidin A as an hourglass-like protein, into artificial membranes, *e.g.* giant unilamellar vesicles or free-standing lipid bilayers. Then, a possible cluster formation of proteins could be tested nearly at the single-molecule level either by fluorescence resonance energy transfer (FRET) or by two color cross-correlation fluorescence correlation spectroscopy (FCS). When using membranes of different thicknesses to create a positive or negative mismatch, one should be able to distinguish between the attractive and repulsive states of two hourglasses or barrels.

References

1 O. G. Mouritsen and M. Bloom, Mattress model of lipid-protein interactions in membranes, *Biophys. J.*, 1984, **46**(2), 141–153.
2 N. Dan, P. Pincus and S. A. Safran, Membrane induced interactions between inclusions, *Langmuir*, 1993, **9**, 2768.
3 N. Dan, A. Berman, P. Pincus and S. A. Safran, Membrane induced interactions between inclusions, *J. Phys. II*, 1994, **4**, 1713.
4 C. Nielsen, M. Goulian and O. S. Andersen, Energetics of inclusion-induced bilayer deformations, *Biophys. J.*, 1998, **74**, 1966–1983.
5 P. Lagüe, M. J. Zuckermann and B. Roux, Lipid-mediated interactions between membrane proteins: a theoretical study based on integral equations, *Biophys. J.*, 2000, **79**, 2867.
6 P. Lagüe, M. J. Zuckermann and B. Roux, Lipid-mediated interactions between intrinsic membrane proteins: dependence on protein size and lipid composition, *Biophys. J.*, 2001, **81**, 276.
7 U. Schmidt, G. Guigas and M. Weiss, Cluster formation of transmembrane proteins due to hydrophobic mismatching, *Phys. Rev. Lett.*, 2008, **101**, 128104.
8 T. Gil, M. C. Sabra, J. H. Ipsen and O. G. Mouritsen, Wetting and capillary condensation as means of protein organization in membranes, *Biophys. J.*, 1997, **73**, 1728–1741.
9 M. Goulian, R. Bruinsma and P. Pincus, Long-range forces in heterogeneous fluid membranes, *Europhys. Lett.*, 1993, **22**, 145.

10 B. J. Reynwar and M. Deserno, Membrane composition-mediated protein-protein interactions, *Biointerphases*, 2009, **3**, FA117.
11 P. A. Kralchevsky and K. Nagayama, Capillary interactions between particles bound to interfaces, liquid films and biomembranes, *Adv. Colloid Interface Sci.*, 2000, **85**, 145.
12 K. M. Palmer, M. Goulian and P. Pincus, Fluctuation-induced forces in stacked fluid membranes, *J. Phys. II*, 1994, **4**, 805.
13 J. M. Park and T. C. Lubensky, Interactions between membrane inclusions on fluctuating membranes, *J. Phys. I*, 1996, **6**, 1217.
14 T. Sintes and A. Baumgaertner, Protein attraction in membranes induces by lipid fluctuations, *Biophys. J.*, 1997, **73**, 2251.
15 T. R. Weikl, Fluctuation-induced aggregation of rigid membrane inclusions, *Europhys. Lett.*, 2001, **54**, 547.
16 B. A. Lewis and D. Engelman, Lipid bilayer thickness varies linearly with acyl chain length in fluid phosphatidylcholine vesicles, *J. Mol. Biol.*, 1983, **166**, 211–217.
17 M. R. R. De Planque and J. A. Killian, Protein-lipid interactions studied with designed transmembrane peptides: role of hydrophobic matching and interfacial anchoring (review), *Mol. Membr. Biol.*, 2003, **20**, 271.
18 A. V. Botelho, T. Huber, T. P. Sakmar and M. F. Brown, Curvature and hydrophobic forces drive oligomerization and modulate activity of rhodopsin in membranes, *Biophys. J.*, 2006, **91**(12), 4464–4477.
19 Y. Yano and K. Matsuzaki, Measurement of thermodynamic parameters for hydrophobic mismatch 1: self-association of a transmembrane helix, *Biochemistry*, 2006, **45**, 3370.
20 F. de Meyer, M. Venturoli and M. Smit, Molecular simulations of lipid-mediated protein-protein interactions, *Biophys. J.*, 1851, **95**, 2008.
21 B. West, F. L. H. Brown and F. Schmid, Membrane-protein interactions in a generic coarse-grained model for lipid bilayers, *Biophys. J.*, 2009, **96**, 101.
22 D. Morozova and M. Weiss, On the role of acylation of transmembrane proteins, *Biophys. J.*, 2010, **98**, 800–804.
23 D. Morozova, G. Guigas and M. Weiss, Dynamic structure formation of peripheral membrane proteins, *PLoS Comput. Biol.*, 2011, **7**, e1002067.
24 M. O. Jensen and O. G. Mouritsen, Lipids do influence protein function-the hydrophobic matching hypothesis revisited, *Biochim. Biophys. Acta*, 2004, **1666**(1–2), 205–226.
25 S. May and A. Ben-Shaul, Molecular theory of lipid-protein interaction and the l-hii transition, *Biophys. J.*, 1999, **76**, 751.
26 J.-B. Fournier, Coupling between membrane tilt-difference and dilation: a new "ripple" instability and multiple crystalline inclusions phases, *Europhys. Lett.*, 1998, **43**, 725.
27 R. D. Groot and P. Warren, Dissipative particle dynamics: bridging the gap between atomistic and mesoscopic simulation, *J. Chem. Phys.*, 1997, **107**, 4423–4435.
28 P. Nikunen, M. Karttunen and I. Vattulainen, How would you integrate the equations of motion in dissipative particle dynamics simulations?, *Comput. Phys. Commun.*, 2003, **153**, 407–423.
29 J. C. Shillcock and R. Lipowsky, Equilibrium structure and lateral stress distribution of amphiphilic bilayers from dissipative particle dynamics simulations, *J. Chem. Phys.*, 2002, **117**, 5048–5061.
30 M. Laradji and P. B. S. Kumar, Dynamics of domain growth in self-assembled fluid vesicles, *Phys. Rev. Lett.*, 2004, **93**, 198105.
31 B. Roux, The calculation of the potential of mean force using computer simulations, *Comput. Phys. Commun.*, 1995, **91**, 275.
32 M. Souaille and B. Roux, Extension to the weighted histogram analysis method: combining umbrella sampling with free energy calculations, *Comput. Phys. Commun.*, 2001, **135**, 40.
33 A. F. Jakobsen, Constant-pressure and constant-surface tension simulations in dissipative particle dynamics, *J. Chem. Phys.*, 2005, **122**, 124901.
34 T. A. Harroun, W. T. Heller, T. M. Weiss, L. Yang and H. W. Huang, Experimental evidence for hydrophobic matching and membrane-mediated interactions in lipid bilayers containing gramicidin, *Biophys. J.*, 1999, **76**, 937–945.

